Validation of Numerical modeling of Supersonic Spatial Flows

A.M. Kharitonov, A.E. Lutsky**, A.M. Shevchenko**

**Khristianovich Institute of Theoretical and Applied Mechanics SB RAS,*
Institutskaja 4/1, 630090 Novosibirsk, Russia
***Keldysch Institute of Applied Mathematics RAS,*
Miusskaja sq. 4, 125047, Moscow, Russia

Abstract

The process of verification and validation includes both the computational and the physical aspects. High reliability of modeling is achieved by estimating the degree of accuracy of a chosen conceptual model in representing the real phenomenon and by comparisons with experimental data.

The adequacy of numerical modeling is evaluated through the following procedures:

- determination of the order of convergence of numerical solutions by comparisons with exact analytical solutions or with the size of the coordinate grid tending to zero;
- evaluation of the sensitivity of the discretization algorithm to various uncertainties: space and time constraints, adaptation of the grid to the model geometry and boundary conditions, etc.

The process of validation involves the following procedures:

- evaluation of the degree of reliability of the chosen numerical and experimental methods;
- evaluation of typical errors of experimental data: nonuniformities of the velocity field, accuracy of measurement equipment, and processing of measured information.

These processes make it possible to analyze the sensitivity of models and their numerical implementation to existing uncertainties. As a result, the degree of reliability of models and methods of numerical modeling can be estimated, and the areas of applicability of various approaches can be determined.

The full paper will give some examples of validation of spatial flows:

- Supersonic flow around a delta wing at an angle of attack;
- Flow between separating aerospace stages;
- Supersonic flow around a ballistic vehicle EXPERT at hypersonic speeds and an angle of attack.

1. Introduction

Intense development of numerical methods of modeling the flow around various vehicles necessitates establishment of rigorous standards for determining the degree of reliability of results and/or the area of their applicability. This especially refers to spatial flows, with models lacking complete adequacy and various assumptions used in numerical simulations. I is well noun, that CFD codes accuracy usually become formed by a validation process because of possible sources of error in the solutions [1]. Numerical validation is necessary because CFD codes provide approximates solutions to the governing equations: they use discrete grids, they employ algorithms that contain numerical dissipation, and they may have nonconvergence errors. On the other hand validation depends on comparisons with well-posed experiments.

Validation experiments are indeed different from traditional experiments, i.e., validation experiments are designed and conducted for

the purpose of model validation. For example, there is a critical need for the detailed characterization of the experimental conditions and the uncertainty estimation of the experimental measurements. For spatial flows, this requires a posteriori error estimation; not just formal error analyses or a priori error estimation. And finally, validation science will require the incorporation of nondeterministic simulations, i.e., multiple deterministic simulations that reflect uncertainty in experimental parameters, initial conditions, and boundary conditions that exist in the experiments that are used to validate the computational models. Otherwise validation implies careful comparisons of results of numerical calculations of the phenomenon under study with experimental data to answer the question: Is the numerical solution physically correct?

Problems of reliability of numerical methods of solving various problems of spatial flows have been discussed at international conferences for the last 15 years [6-11]. The possibility of development of databases containing test cases for comparisons of numerical solutions with experimental data is considered [12]. Such databases stimulate

further development of the methodology of numerical and physical research and lead to a higher level of aerothermodynamic data, as applied to in-flight conditions, with the aim of determining uncertainties.

A specific problem of the methods developed is the low accuracy of calculating flows with shock wave-boundary layer interaction leading to formation of separation regions.

Adequate numerical modeling of complex flows in the vicinity of spatial configuration requires a strategy for verification and validation of software products being developed. As numerical realizations are only approximations of real flows and, hence, only approximations of reality, their reliability has to be estimated via known procedures of *verification* and *validaton.* To use these procedures successfully, one has to understand the difference between them.

As was stated in [6], *verification* is the process of determining the degree of adequacy and the level of accuracy of numerical modeling of a particular conceptual model, while *validation* is the process of determining the degree to which a model is an accurate representation of the real phenomenon and/or shows how accurately the chosen conceptual model describes the examined flow through comparisons of numerical and experimental data. These procedures are schematically shown in fig. 1.

Hence, the process of verification and validation includes both the computational and physical aspects. High reliability of modeling is achieved by estimating the degree of accuracy of a chosen conceptual model in representing the real phenomenon and by comparisons with experimental data.

The adequacy of numerical modeling is evaluated through the following procedures:

- determination of the order of convergence of numerical solutions by comparisons with exact analytical solutions (if they exist) or with the size of the coordinate grid tending to zero;
- evaluation of the sensitivity of the discretization algorithm to various uncertainties: space and time constraints, adaptation of the grid to the model geometry and boundary conditions, etc.

The process of validation involves the following procedures:

- evaluation of the degree of reliability of the chosen numerical and experimental methods;
- evaluation of systematic errors of experimental data: non- uniformities of the velocity field, effect of the test-section walls and supporting devices, and accuracy of measurement equipment and processing of measured information. It is also necessary to know the level and scale of turbulence at the test-section entrance.

In accordance with [8,13], validation of results of numerical simulations implies a comparative analysis of the physical model and all uncertainties, including uncertainties associated with initial and boundary conditions from the physical and computational viewpoints.

Uncertainties are usually inherent in both numerical and experimental modeling. Numerical modeling involves uncertainties associated with 1) insufficient correspondence between the theoretical and numerical models, 2) insufficient accuracy of computations, 3) inaccurate modeling of the phenomenon, 4) influence of external phenomena, and some others. Wind-tunnel modeling implies overcoming difficulties related to 1) effects of interference of phenomena, 2) insufficient measurement accuracy, 3) insufficient number of tests, 4) choosing and defining a particular test program, etc. The critical difference between numerical and physical modeling is the degree of modeling of the phenomenon and insufficiency of measurements.

Thus, careful verification and validation allows researchers to analyze the sensitivity of models and their implementations to existing uncertainties. As a result, the degree of reliability of models and methods of numerical modeling can be estimated, and the areas of applicability of various approaches can be determined.

Several examples of validation for spatial flows are given below: 1) the flow around a delta wing at an angle of attack, 2) the flow around two separating stages of an aerospace vehicle and axisymmetric Re-entry Test bed (EXPERT) at hypersonic speeds.

2 **Supersonic flow around a delta wing at an angle of attack**

Regimes of the flow around a delta wing are characterized by the number, size, and position of streamwise vortices and internal shock waves. Owing to this variety of features, this class of flows is a good test case for methods of calculating complex spatial flows under development. For this purpose, the Khristianovich Institute of Theoretical and Applied Mechanics of the Siberian Branch of the Russian Academy of Sciences (ITAM SB RAS) and the Keldysh Institute of Applied Mathematics of the Russian Academy of Sciences (KIAM RAS) performed a comprehensive numerical and experimental study of the flow field on the leeward side of the delta wing [13÷21]. The flow around the delta wing was numerically modeled with the use of the spatial steady Euler equations and unsteady Navier-Stokes equations. An algorithm was developed, which allowed the Euler and Navier-Stokes models to be simultaneously used in different blocks. A grid with six blocks was developed, and the zonal approach was applied with the use of algorithms of parallelization of computations on high-resolution grids containing up to 640 nodes along the wing half-span. Such an algorithm facilitates grid generation in areas of different shape, allows some solution discontinuities to be identified in the form of moving boundaries of areas, and makes it possible to use different physical models in different blocks.

Advanced methods used in experiments include optical visualization of the limiting streamlines on the model surface by the oil-film method, visualization of the spatial pattern of the flow by the laser sheet technique, measurement of pressure distributions over the model surface, and measurements of fields of gas-dynamic parameters with the use of a rake with five-channel pneumometric probes. Figure 2 shows the delta wing geometry and its basic parameters.

The analysis of the results obtained and the validation of the method of calculations within the framework of the Euler equations through comparisons with experimental data are illustrated in Fig. 3. It is seen that numerical modeling predicts the flow regime with formation of the primary and secondary vortices and also a system of weak compression waves above the primary vortex on the leeward surface. The shock wave under the primary vortex is not identified, which may be caused by insufficient grid resolution.

There are grounds to believe that the use of a larger number of grid nodes will allow this shock wave to be resolved. At the same time, the neglect of the turbulent state of the boundary layer leads to violation of flow conicity, thus, making the flow more sensitive to pressure gradients on the wing surface. Hence, it is necessary to solve this problem with the use of the Navier-Stokes equations and appropriate turbulence models. It was shown [15] that such an approach provides adequate simulation of the flow topology on the wing surface and in its vicinity and predicts reasonable values of gas-dynamic parameters.

Verification and validation of the numerical realization of solving the problem considered stimulated the use of a hybrid method of numerical modeling, combining the Euler and Navier-Stokes models.

The Navier-Stokes model was used in two out of six blocks adjacent to the wing surface, and the Euler model was used in the remaining four blocks. The patterns of the surface streamlines calculated by the Navier-Stokes and Euler equations are compared in fig. 4. Figure 5 shows the spanwise distributions of the pressure coefficient in two cross sections of the wing in comparison with experimental data.

The calculations of the flow around the delta wing and comparisons of the results obtained with experimental data demonstrate fairly good agreement with the Navier-Stokes calculations.

The differences in pressure distributions and in formation of vortex structures above the wing, calculated by the Navier-Stokes and Euler equations, are illustrated in fig. 6.

Thus, the process of numerical modeling accompanied by careful validation allows the area of applicability of the Euler model for this class of flows to be determined. As a consequence, perfect software products can be developed to study the specific features and to calculate complex spatial flows.

3 **Flow between separating aerospace stages**

In this case, two-stage-to-orbit systems the second stage is the orbiter, and the first stage equipped by an air-breathing engine ensures separation of the stages in the range of Mach numbers of 6÷12 at altitudes of ~ 30 km and, hence, at high dynamic pressures. Under these conditions, the aerodynamic interference between the stages exerts a significant effect on the separation maneuver safety.

In the general case, the flow around separating stages is a complicated three-dimensional unsteady gas-dynamic problem. As it is shown in fig. 7, the flow between the stages is accompanied by interaction of incident and reflected shock waves and expansion waves with each other and with boundary layers.

This class of flows was intensely studied, and results were reported in many publications, including [23-34]. The pressure fields in the flow around two bodies of revolution and interference between these bodies and a flat plate were analyzed in detail in [22].

Aerodynamic interference of separating generic two-stage winged systems was studied numerically and experimentally in [23-28]. Adequate numerical simulation of such flows is impossible without profound understanding of the physical pattern of interaction of the stages. Therefore, a comprehensive aerophysical experiment was performed in a supersonic wind tunnel based at ITAM SB RAS at a Mach number M_∞=3 and Reynolds number per meter Re_1= 35 10^6 m^{-1}.

The experiment included measurement of integral and distributed characteristics in a wide range of relative positions of the separating stages.

The models of the first and second stages are combinations of an axisymmetric cone-cylinder body with a flat tapered wing with sharp leading and trailing edges (fig. 8). The sweep angle of the leading edge of the wing is $\chi = 53^\circ$. The wing has a hexagonal profile with a constant spanwise thickness equal to 4% of the wing chord. The second stage model is a halved copy of the first stage. Modeling of separation of the stages within the ranges $\Delta z = D \div 3D$ and $\Delta x = -0.5D \div 1.5D$ was provided by a special device. The angle of attack of the second stage was changed simultaneously with the change in the angle of attack of the first stage within the range $\alpha = 0 \div 10^\circ$.

An analysis of uncertainties and their possible contributions to the integral error allows one to estimate the maximum deviations of aerodynamic coefficients (they stay within the interval ±0.01 ÷ 0.03), which allows the differences between numerical and experimental data to be found with high reliability.

Numerical modeling of separation of the stages was performed to determine the area of applicability of gas-dynamic equations for this class of problems. The algorithm of solution of three-dimensional steady Euler equations was implemented at KIAM RAS on multiprocessor computing systems and was described in detail in [26-28].

An example of calculated and experimental values of the pressure coefficient on the surfaces of the stages in the plane of symmetry is shown in fig. 9. The character of the dependences $C_p(x)$ reflects the above-mentioned features of the flow in the space between the stages. Satisfactory qualitative and quantitative agreement is observed everywhere between the calculations and experiments in terms of the coordinate of arrival of the bow shock wave from the second stage on the first stage and the values of pressure in this region. There are significant differences, however, especially at $\alpha > 0$, in the values of pressure directly behind the inflection of the body (cross section x=3.5D) of the first stage.

The calculated pressure distributions at $\Delta z = 1.5D$, where the governing factors of the influence of the second stage on the first stage are the bow shock wave and the expansion fan from the junction of the nose part with the body, are also in good agreement with the experiment (figs. 9a and 9b).

As the nose part and the major part of the body of the second stage at $\Delta z = 1$ is located in the conical flow field of the first stage, the positive phase of excess pressure is additionally realized on a significant part of the lower surface of the second stage (fig. 9c). Under the influence of the expansion fan from the first stage, however, the pressure on the second stage decreases, and a region with the negative phase of excess pressure is formed. The pressure increases again when the shock wave emanating from the wing arrives on the lower part of the body.

As the angle of attack increases, the positive deflections of the conical flow field become smaller, and the effect of the expansion fan becomes more pronounced. Correspondingly, the positive phase of excess pressure decreases, and the negative phase increases (fig. 9d). At both angles of attack, significant differences between the calculations and experiments are observed in the region of the negative phase of excess pressure. This can be attributed to the arrival of the shock wave from the second stage wing on the lower part of the body and the corresponding increase in pressure, which is predicted by calculations to be much closer to the base region than it follows from the experiment. Apparently, these differences are associated with insignificant density of the computational grid. Clearly identifying the features of the flow around the first stage, the grid is insufficient for adequate calculation of the flow around the second stage because of the smaller size of the latter. The second reason for these differences may be the insufficient adequacy of the mathematical model chosen for this flow, because the model does not take into account the specific features of the boundary-layer flow. As was shown in [27], the angle of shock-wave reflection from the surface in the boundary layer is noticeably greater in the experiment than in the calculation. This fact is largely responsible for the differences in the subsequent flow regions. If the near-wall region is calculated by the Navier-Stokes equations with an appropriate turbulence model, good agreement between the calculation and experiment can be expected.

Thus, an analysis of results of three-dimensional inviscid Euler computations with the use of the zonal approach and validation of these results by experimental data confirm the possibility of predicting a complicated structure of supersonic flows in the vicinity of separating Another example of a two-stage-to-orbit aerospace system is the ELAC-EOS concept developed at the Institute of Aerodynamics at the Aachen Technical University. This geometry configuration (fig.10) is as close to the real one as possible. The results of vast numerical and experimental studies of the ELAC-EOS two-stage aerospace system were obtained together with the Aerodynamic Institute at the Aachen Technical University,
Munich Technical university, and ITAM SB RAS in Novosibirsk. They are described in [29-34]. The characteristics of the ELAC-EOS models were also studied in the T-313 supersonic wind tunnel of ITAM SB RAS at $M_\infty = 4.0$ and $Re=4.8\cdot10^6$. The following parameters were varied:

- distance between the models h/L=0.225, 0.325, and 0.450;
- angles of sideslip of the second stage $\Delta\beta=0°$, 2°, and 4°;
- angles of fixation of the second stage with respect to the first stage $\Delta\alpha=0°$, 2°, and 5°;
- angles of rolling $\Delta\phi=0°$, 2°, and 4°.

The angles of attack of both models were simultaneously changed in the range $\alpha=0\div6°$ with a step of 1° for each parameter being fixed.

Separation of the ELAC-EOS stages was calculated by three-dimensional laminar Navier-Stokes equations, which were solved by the finite-volume method in curvilinear coordinats including structured and unstructured blocks. For more careful verification and validation of the numerical method, special experiments were performed to study the flow during separation of the EOS orbital stage from a flat plate.

As an illustration, the Schlieren picture of on interaction case is compared in fig. 11 with the calculated static pressure distribution on the surface of the second stage.

As in the experiment, the calculation (fig. 11b) at a distance h/L=0.150 and angle of attack α=0 predicts the position of the bow shock wave from the model and the reflected shock wave from the flat plate, which is then incident on the rear part of the model in the vicinity of its base region. Thus, a comparison between the calculation and experiment shows that the calculation correctly reproduces all basic features of the flow.

The calculated pressure distribution on the flat plate is compared with experimental results in fig. 12. It is clearly seen that small differences are observed only in a local region of incidence of the bow shock wave onto the plate and in the vicinity of arrival of the oblique shock wave from the wing.

A visual analysis of the Schlieren pictures of interaction between the stages showed that the main factors of influence of the first stage on the second stage are the bow shock wave of the first stage, the expansion fan induced by flow deflection when the flow enters the cavity for the second stage the barrel shock wave induced by flow turning along this cavity, and (in some cases with the minimum distance between the stages) the expansion fan induced by flow deflection at the maximum thickness cross section of the first stage. There are only two factors of influence of the second stage on the first stage: the bow shock wave of the second stage and the shock waves induced by the wings of the second stage.

Depending on the geometry of the first and second stages and their relative positions, the following events are possible:

- negative interference region, where the second stage completely loses its lifting properties;
- formation of reverse changes of the pitching moment owing to displacement of the center of pressure upstream or downstream during separation of the second stage.

These and other interference effects can substantially influence the separation maneuver safety.

4 **Supersonic flow around a ballistic vehicle EXPERT at hypersonic speeds and an angle of attack**

The experiments were performed in two hypersonic wind tunnels: blowdown wind tunnel T-313 and adiabatic compression wind tunnel T-303 at Khristianovich Institute of Theoretical and Applied Mechanics SB RAS.

With the aim of possible refinement of flow parameters, the calculations was performed by the Navier-Stokes equations with the *k-ε RNG* model of turbulence. The computed pressure distribution at a zero angle of attack is shown in fig. 14 In particular, the Euler calculations made it possible to estimate the flow parameters directly ahead of the flap and the level of pressure on the flap. Thus, the Mach number ahead of the flap is $M_1 = 2.8$, and the pressure drop on the shock wave is $p_2 / p_1 \sim 3.5$.

A comparison of this level with the simplest estimates of the critical pressure drop $\bar{p}_{kr} = 1 + 0.5M_1 = 2.4$ for the turbulent boundary layer indicates the possibility of separation of the boundary layer owing to its interaction with the shock wave. Subsequent Navier-Stokes calculations confirmed the presence of the separation region in the vicinity of the flap. It should also be noted that the results of viscous and inviscid predictions for the pressure distributions outside the separation region are almost identical. Figure 15 shows the drag coefficient C_D as a function of the Mach number for
the angle of attack $\alpha = 0$ and angles of rolling $\gamma = 0$ and 45°, which was obtained on the basis of measurements performed in the T-205, T-313, and AT-303 wind tunnels in the entire range of the Mach numbers considered: $M_\infty = 0.6 \div 16$. For comparison, this figure also shows the experimental data obtained in VKI wind tunnels and also the results of numerical calculations at $\alpha = 5°$ [35]. Satisfactory agreement of experimental data obtained in different wind tunnels can be noted. The observed difference with the numerical calculation is apparently caused by the fact that the calculation was performed for the case with $\alpha = 5°$.

Thus, the examples of validation of numerical methods for calculating complex spatial flows considered above and many others show that this procedure is extremely important.

It allows the area of applicability of numerical methods to be determined and their reliability
and accuracy to be improved. For these reasons, the validation procedure should undoubtedly become a necessary attribute of numerical methods under development.

The information obtained can be used for validation of numerical methods [29-31].

This work was sponsored by RFFI in frame of the projects № 03-01-00249, 06-01-00774, 12-01-00806.

References

1. Wilcox D.C. Reassessment of the scale determining function for advance turbulence models. AIAA J. 1988. Vol.19. No. 2.

2. Launder B.E., Sharma B.I. Application of the energy dissipation model of the turbulence to the calculation of flow near a spinning disc. Letters in Heat and Mass Transfer. 1974. Vol. 1.
3. Lam C.K.G., Bremhorst K.A. Modified form of the (k-ω) model predicting wall turbulence. J. Fluids Eng. 1981. Vol. 103.
4. Menter F.R. Improved two-equation (k-ω) turbulence models for aerodynamic flows. NASA TM-103975. 1992.
5. Kurbatskii A.F. Introduction into Modeling of Turbulent Transport of Momentum and Scalar. GEO. 2007.
6. Unmeel B. Mehta. Guide to credible computational fluid dynamics simulations. AIAA Paper No. 95 – 2225. 26th AIAA Fluid Dynamics Conference. 1995.
7. Joseph G. Marvin. CFD Validation experiments for hypersonic flows. AIAA Paper No.- 92 – 4024. 17th Aerospace Ground Testing Conference. 1992.
8. William L. Oberkampfa, Timothy G. Trucanob. Verification and validation in computational fluid dynamics. Progress in Aerospace Sciences 38, 2002.
9. Jean M. Delery. A strategy for code validation in high Mach number flows: The experimentalist point of view. Proceedings of West East High Speed Flow Fields Conference 2003. P. 1-12.
10. J.-A. Desideri, M. Marini, J.Periaux. Validation databases in mechanics: From the European space shuttle program Hermes to the European thematic network Flownet. Proceedings Flow Dynamics and Aeronautics New Challenges Conference Dedicated to Pierre Perrier. 2003. P. 535-546.
11. Bosnyakov S.M. Concept of the EWT-TsAGI software product and basic stages of its development. Proceedings TsAGI Intern. Conf. 2004.
12. Marini M. An example of CFD codes verification and validation in aeronautics and turbo machinery: The European Flownet database project. Proceeding of the EWHSFF Conference Beijing, China, October 19 22, 2005.
13. Zabrodin A.V., Chernoguzov A.S., Lutsky A.E., Kharitonov A.M., Shevchenko A.M. Verification of numerical modeling of spatial flows on the leeward side of a delta wing. Proceedings XVIII Intern. School, Saratov, August 27 – September 1, 2007.
14. Brodetsky M.D., Zabrodin A.V., Lutsky A.E., Kharitonov A.M., Shevchenko A.M. Numerical and experimental modeling of supersonic flow regimes around a delta wing. Thermophys. Aeromech., 2004. Vol. 11. No. 2. P. 167-188.
15. Brodetsky M.D., Zabrodin A.V., Lutsky A.E., Kharitonov A.M., Shevchenko A.M. Regimes of a supersonic flow around a delta wing. Experimental and numerical modeling. Proceedings XV All-Russian Conf. "Theoretical basis and design of numerical algorithms for solving problems of mathematical physics as applied to multiprocessor systems" devoted to the memory of K.I.Babenko. Abrau-Dyurso. 2004.

16. Brodetsky M.D., Kharitonov A.M., Krause E., Pavlov A.A., Nikiforov S.B., Shevchenko A.M. Supersonic lee-side flow topology on delta wings revisited. J. Experiments in Fluids. 2000. Vol. 29. P. 592-604.
17. Lutsky A., Shevchenko A, Zabrodin A. Supersonic lee-side flow over delta wings. Proceedings of the East West High Speed Flow Field Conference Beijing, China, October 19 22, 2005.
18. Brodetsky M.D., Kharitonov A. M., Shevchenko A.M, Chernogusov A., Lutsky A.E., Zabrodin A.V. Validation of CFD Simulation of a Supersonic Lee Side Flow Over Delta Wings // 1th European Conference for Aerospace Sciences EUCASS July 4-7th, 2005 – Moscow.
19. Brodetsky M.D, Kharitonov A. M. Shevchenko A.M., Lutsky A.E., Zabrodin A.V. Supersonic Lee-Side Flow over a Delta Wing // EWHSF Conference Beijing, China, October-2005.
20. Brodetsky M.D. A.M. Kharitonov, N.P. Shevchenko A.M., Zabrodin A.V., Lutsky A.E. Supersonic Lee-Side Flow over a Delta Wing. Proceedings Europe-Russia workshop, November 2006, Barcelona (Spain).
21. Kharitonov A.M, Lutsky A.E., Shevchenko A.M. Investigation of supersonic vortex cores above and behind of a wing. Proceedings of the 2th European Conference for Aerospace Sciences-EUCASS July 1-6th, 2007, Brussels.

22. Brodetsky M.D., Derunov E.K., Zabrodin A.V., Lutsky A.E. Comparison of numerical and experimental investigations of the flow around combinations of two bodies of revolution. Thermophys. Aeromech., 1995. Vol. 2. No. 2. P. 97-102.

23. Bonnefond T., Kharitonov A.M., Brodetsky M.D., Vasenyov L.G., Adamov N. Separation of winged vehicles in supersonics. AIAA Paper 95-6092, 1995.

24. Adamov N.P., Bonnefond T., Brodetsky M.D., Vasenev L.G., Derunov E.K., Kharitonov A.M. Experimental study of aerodynamic interference of two-stage winged system during separation. Part 1. Experimental technique. Distributed aerodynamic characteristics. Thermophys. Aeromech. 1996. Vol. 3. No. 3.

25. Adamov N.P., Bonnefond T., Brodetsky M.D., Vasenev L.G., Derunov E.K., Kharitonov A.M. Spatial supersonic flows during separation of two-stage aerospace systems. J. Appl. Mech. Tech. Phys. 1997. No. 1.

26. Brodetsky M.D., Derunov E.K., Kharitonov A.M., Lutsky A. E. , Zabrodin A. V. Interference in a supersonic flow around a combination of bodies. Proceedings of the First Europe-US High Speed flow field Database Workshop, Part II, Naples, Italy, November 12-14, 1997.

27. Adamov N.P., Brodetsky M.D., Lutsky A.E., Kharitonov A.M., Shevelko A.V. Calculation of a supersonic flow around separating winged bodies. Preprint No. 12, Keldysh Inst. Appl. Math., Moscow. 1999.

28. Adamov N.P., Brodetsky M.D., Kharitonov A.M., Zabrodin A.V., Lutsky A.E. Numerical and physical modeling of a supersonic flow around separating winged bodies. Thermophys. Aeromech. 2000. Vol. 7. No. 1.

29. Krause E., Limberg W., Kharitonov A.M., Brodetsky M.D., Henze A. An investigation of the ELAC1 configuration at supersonic speeds. J. Experiments in Fluids. 1999. Vol. 26. P. 4423-4436.

30. Kharitonov A.M., Brodetsky M.D., Vasenyov L., Adamov N., Breitsamter C., Heller M. Investigation of aerodynamic characteristics of the models of a two-stage aerospace system during separation, Final report, SFB 255, 2000.

31. Kharitonov A.M., Brodetsky M.D., Henze A., Schröder W., Heller M., Sachs G., Breitsamter C., Laschka B. Experimental and numerical analysis of supersonic flow over ELAC-configuration. In: Basic Research and Technologies for Two-Stage-to Orbit Vehicles. WILEY-VCH Verlag GmbH & Co. KGaA. 2001.

32. Adamov N.P., Brodetsky M.D., Vasenev L.G., Kharitonov A.M. Supersonic spatial flows during separation of two-stage aerospace systems. Presentation at VIII All-Russian Forum on Theoretical and Applied Mechanics. Perm. August 23-29, 2001.

33. Kharitonov A.M. Some problem of gas dynamics of hypersonic flying vehicles. Lecture on the scientific conference “Fundamentals of future two-stage space transportation systems.” Munich. October 9-10, 2003.

34. Kharitonov A. M., Adamov N. P., Brodetsky M. D., Lutsky A. E. , Zabrodin A. V. Spatial supersonic flows over separating winded bodies. Numerical and experimental simulation. ECCOMAS-2004, 24-28 July, Juvaskula, Finland, Volume 2 and CD.

35. Shettino A. et al. Aerodynamic and aerothermodynamic data base of EXPERT capsule. West-East high speed flow field conference, 19-22 November 2007, Moscow, Russia.

Figures:

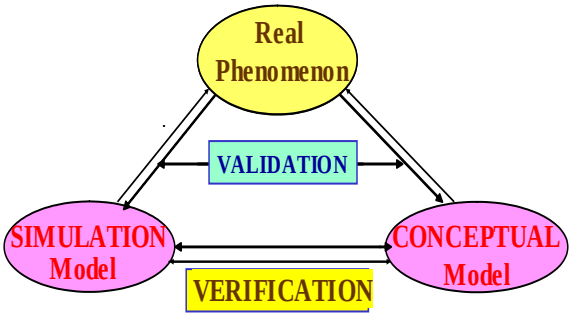

Figure 1.

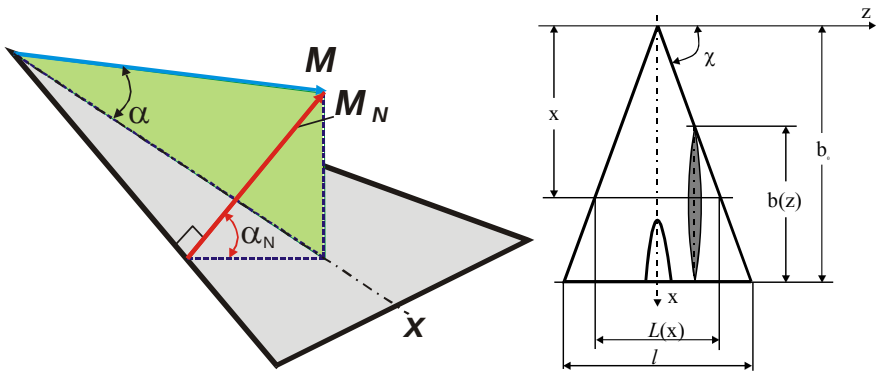

Normal angle of attack

$$\alpha_N = arctg(tg\alpha / \cos\chi)$$

Normal Mach number

$$M_N = M\cos\chi(1-\cos^2\alpha\sin^2\alpha)^{1/2}$$

Figure 2. Delta wing with a sweep angle $\chi = 78^\circ$, 3% symmetric parabolic profile.

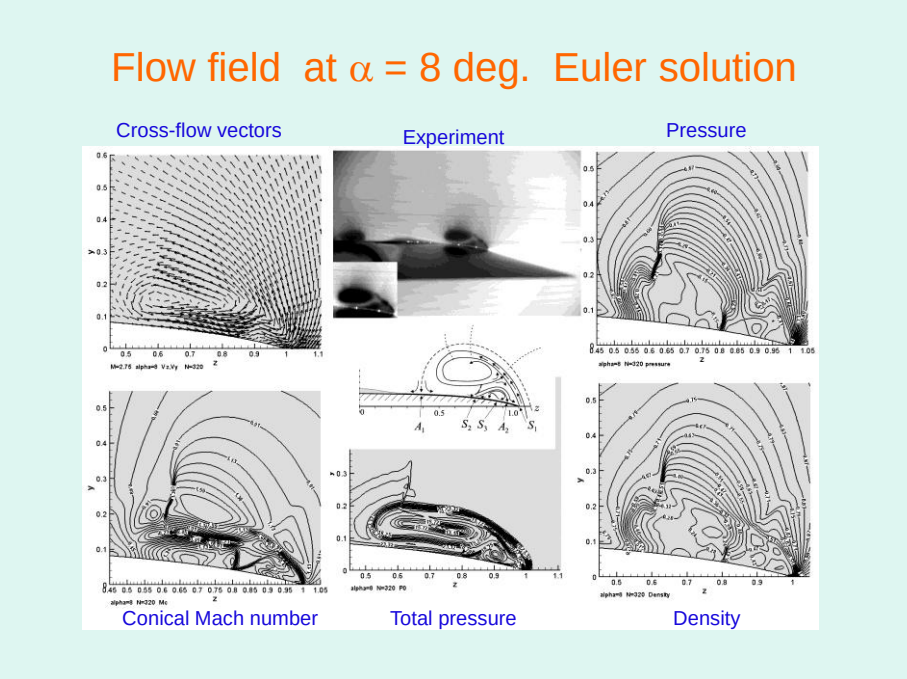

Figure 3

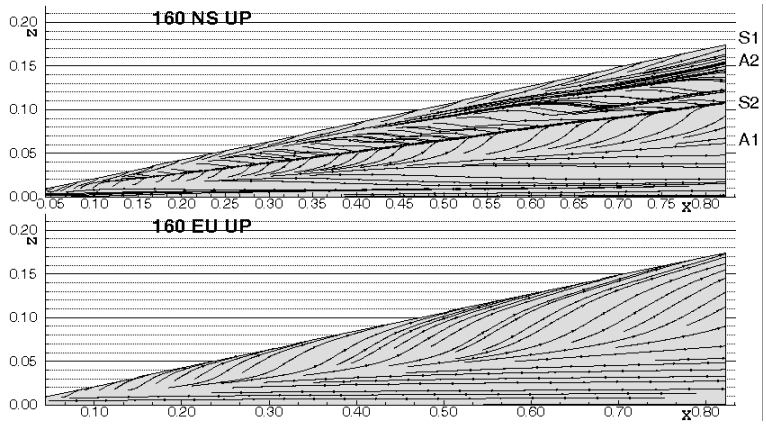

Figure 4

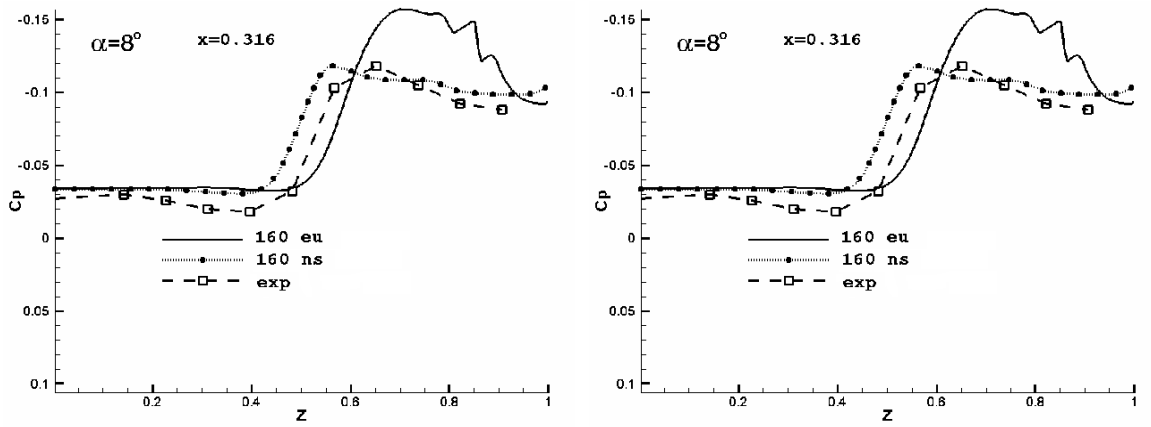

Figure 5

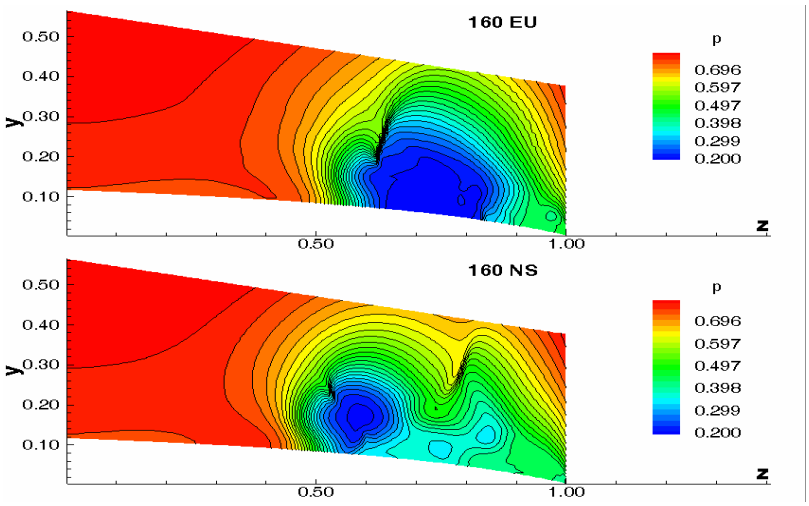

Figure 6

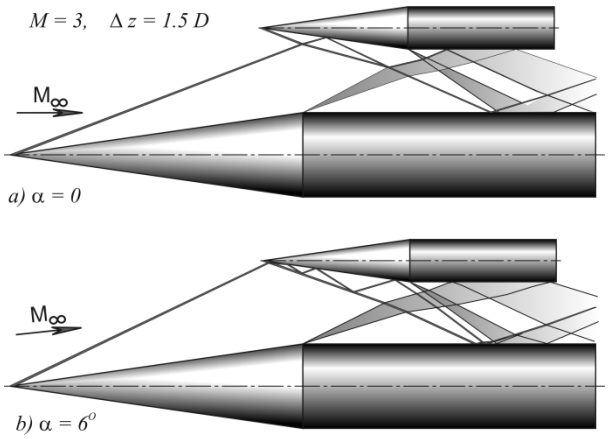

Figure 7

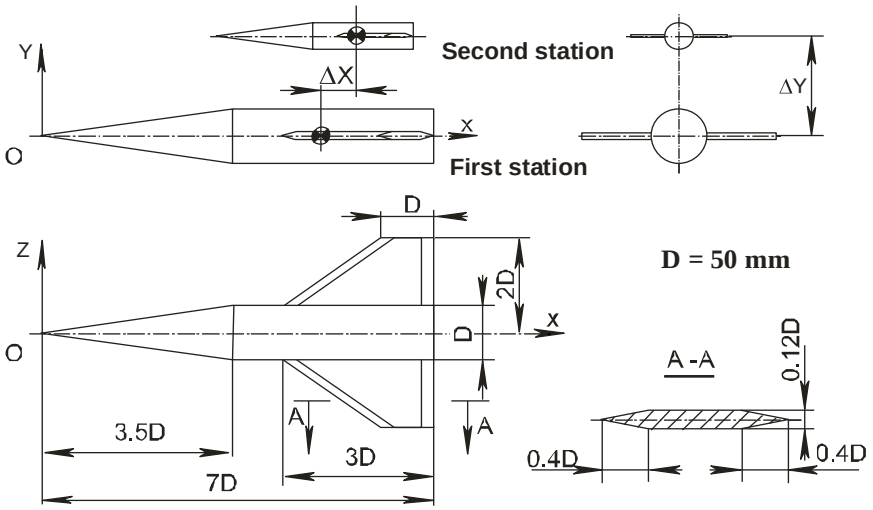

Figure 8

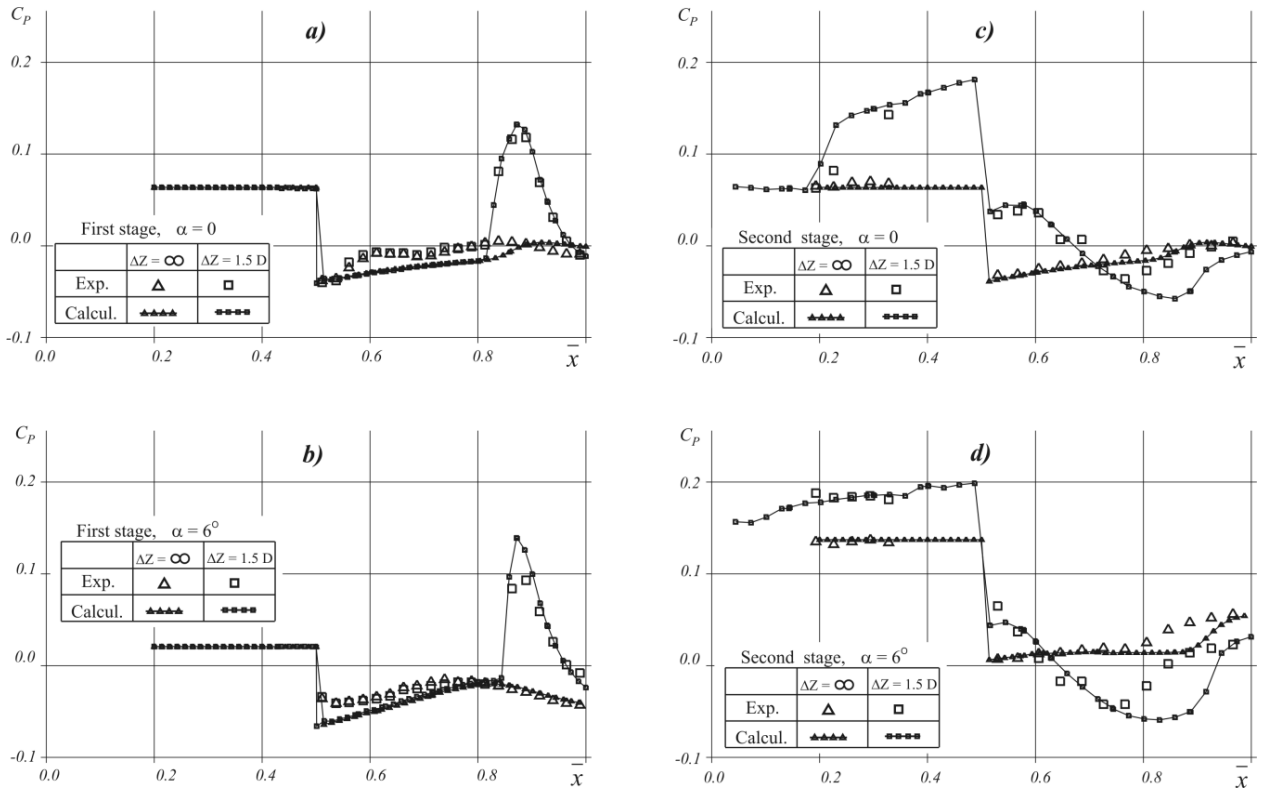

Figure 9

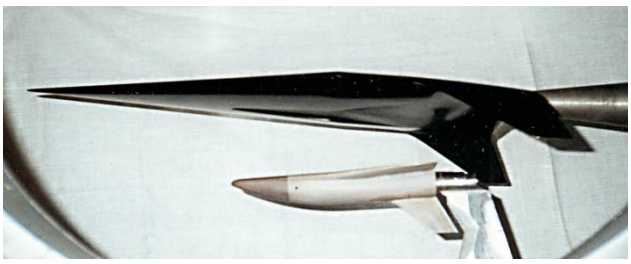

Figure 10

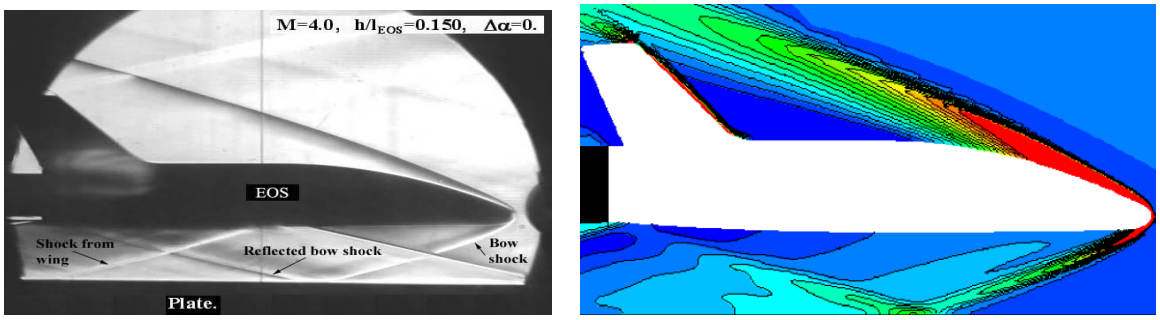

a) b)

Figure 11. a) Schlieren picture; b) Static pressure distribution (calculation)

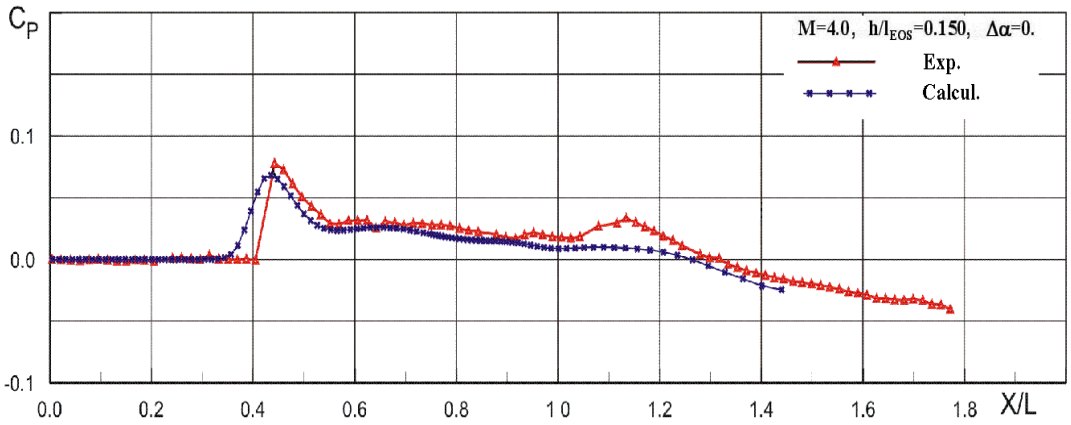

Figure 12

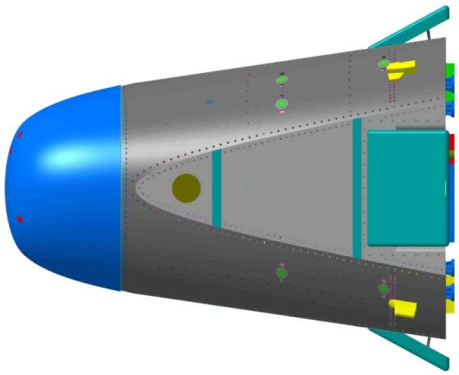

Figure 13 European Experimental Re-entry Test bed (EXPERT)

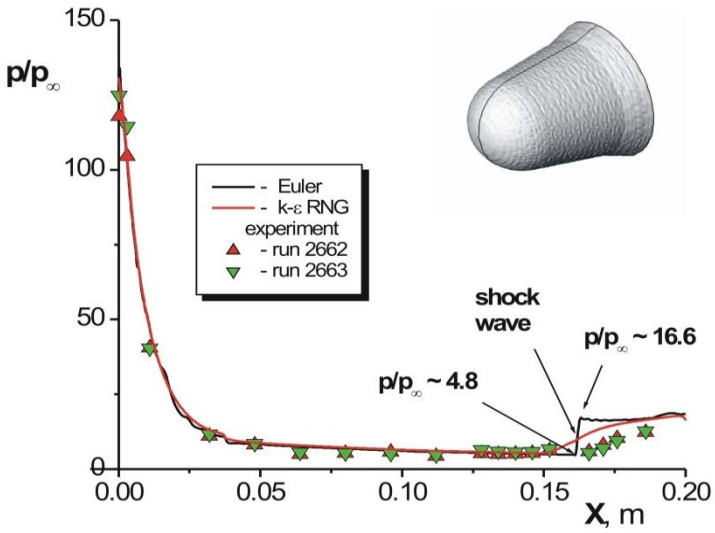

Figure 14

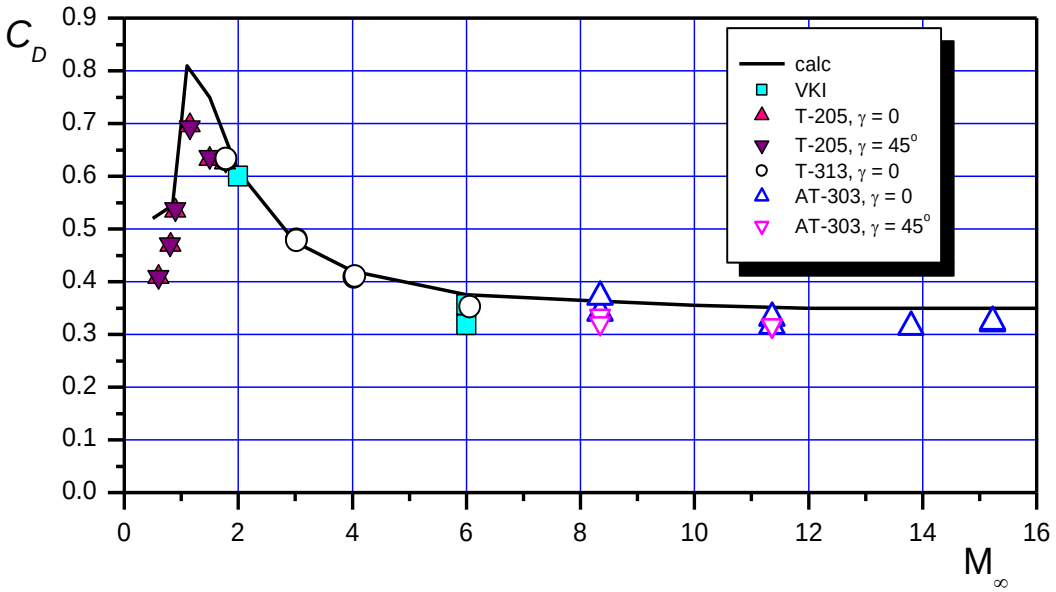

Figure 15 Drag coefficient versus the Mach number in different wind tunnels.